

# Analytical-Numerical Solutions of Photo-Thermal Interactions in Semiconductor Materials

Ibrahim Abbas<sup>1\*</sup> and Aatef D. Hobiny<sup>2</sup>

<sup>1</sup>Department of mathematics, Faculty of Science, Sohag University, Egypt

<sup>2</sup>Department of Mathematics, Faculty of Science, King Abdulaziz University, Saudi Arabia

Received: 21 Dec. 2020, Revised: 22 Feb. 2021, Accepted: 7 Mar. 2021

Published online: 1 May 2021

**Abstract:** Analytical and numerical solutions are two basic tools in the study of photothermal interactions problems in semiconductor medium. This paper is devoted to a study of the photothermal interaction in semiconductor media in the context of the coupled photo-thermal theory. The governing relations are expressed in Laplace transforms domain and solved in the domain by the eigenvalue scheme. The numerical solution is obtained by using the implicit finite difference method (IFDM), the studied fields are obtained numerically and presented graphically. A comparison between the numerical solutions and the analytical solution are obtained. It is found that the implicit finite difference method (IFDM) is applicable, simple and efficient for such problems.

**Keywords:** Finite difference method; Laplace transforms; Semi-conductor medium; eigenvalue approach.

## Nomenclature

$T = T^* - T_o, T^*$	the variations of temperature
$T_o$	the reference temperature
$t$	the time
$u_i$	the displacement components
$\rho$	the density of material
$c_e$	the specific heat at constant strain,
$\tau$	the lifetime of photo-generated carrier,
$N = n - n_o, n_o$	the carrier concentration at equilibrium,
$\gamma_n = (3\lambda + 2\mu)d_n,$ $d_n$	the electronic deformation coefficient,
$k = \frac{\partial n_o}{\partial T}$	the coupling parameter of thermal activation
$K$	the thermal conductivity
$\gamma_t = (3\lambda + 2\mu)\alpha_t, \alpha_t$	the linear thermal expansion coefficients
$\sigma_{ij}$	the components of stresses,
$D_e$	the carrier diffusion coefficient,
$\lambda, \mu$	the Lamé's constants,

\*Corresponding author e-mail: [ibrabbas7@science.sohag.edu.eg](mailto:ibrabbas7@science.sohag.edu.eg)

$T_1$	the constant temperature
$t_f$	the final value of time
$x_f$	the final value of length
$s_b$	the speed of recombination on the surface
$\Omega$	the exponent of the decayed heat flux

## 1 Introduction

The models of bodies explained the properties of the internal structure of medium when used the secondly law of thermodynamic with the development of semi-conductor integrated circuit technology and solid-state sensors technology have been widely used in several fields. The significance of semiconductor material is due to its recent uses in several interesting application, essentially in modern technology upon new energy alternative. Previously, micro-mechanical structures of the thermoelasticity and plasma field are analyzed theoretical and experimental as in Todorovic et al. [1-3]. In these investigates, the theoretically analysis to depict these two-phenomena that give information about the attributes of carriers recombination and transports in the semiconductors materials. Abd-Alla et al. [4] studied the solutions of the transient coupled thermoelastic of an annular fins by the implicit finite-difference technique. Mukhopadhyay and Kumar [5] applied the finite difference technique to study the generalized thermoelasticity problem of annular cylinders with variable material properties. Abd-Alla et al. [6] studied the effects of nonhomogeneous in an isotropic cylinder under magnetic field. Patra et al. [7] used the finite difference technique to study the computational model on thermoelastic analysis with the magnetic field in a rotating cylinder. Abd-Alla et al. [8] studied the effects in a thermoelastic annular cylinder using the finite difference method. Lotfy et al. [9] discussed the responses of Thomson and electro-magnetic influences of semi-conductor material casued by laser pulses under photo-thermoelastic excitation. Abbas et al. [10] presnted th solutions of photo-thermal interaction in a semiconducting materials with cylindrical hole and variable thermal conductivity. Alzahrani [11] investigated the effects of variable thermal conductivity in semi-conductor materiale. Lotfy et al. [12] investigated the influences of variable thermal conductivity in semiconductors mediums with cavity under fractional-order magneto-photothermal models. Lotfy et al. [13] studied the electro-magnetic and Thomson effects through the photo-thermal transport process of semiconductor material. Hobiny and Abbas [14] discussed the photothermoelasticity interaction in a two-dimension semiconducting plane under Green-Naghdi theory. Alzahrani and Abbas [15] discussed the photothermoelasticity interactions in a two-dimentionn semiconductors mediums without energy dissipation. Several authors [16-30] used the venous thermoelastic theories to get the solutions of several problems.

The present work is devoted to study the photothermal interaction in a semiconductor material by using the numerical and analytical methods. Numerical outcomes for the displacement, the temperature, the carrier density and the stress distributions are presented graphically. Finally, the accuracy of the finite difference method was validated by the comparing between the numerical and the analytical solutions for all physical fields.

## 2 Basic Equations

The basic equations in an isotropic semi-conductor material in the absence the thermal sources and the body force are taken as in [31-33]:

$$\mu u_{i,jj} + (\lambda + \mu)u_{j,ij} - \gamma_n N_{,i} - \gamma_t T_{,i} = \rho \frac{\partial^2 u_i}{\partial t^2} \quad (1)$$

$$D_e N_{,jj} - \frac{N}{\tau} + \frac{k}{\tau} T = \frac{\partial N}{\partial t}, \quad (2)$$

$$(KT_{,j})_j + \frac{E_g}{\tau} N - \gamma_t T_o \frac{\partial u_{jj}}{\partial t} = \rho c_e \frac{\partial T}{\partial t}. \quad (3)$$

$$\sigma_{ij} = (\lambda u_{k,k} - \gamma_t T - \gamma_n N) \delta_{ij} + \mu (u_{i,j} + u_{j,i}), \quad (4)$$

Let us consider an unbounded isotropic semiconductor medium, whose state can be expressed as a function of the spatial variable  $x$  and time  $t$ , hence the relations (1)-(4) can be given by:

$$(\lambda + 2\mu) \frac{\partial^2 u}{\partial x^2} - \gamma_t \frac{\partial T}{\partial x} - \gamma_n \frac{\partial N}{\partial x} = \rho \frac{\partial^2 u}{\partial t^2}, \quad (5)$$

$$D_e \frac{\partial^2 N}{\partial x^2} - \frac{N}{\tau} + \frac{k}{\tau} T = \frac{\partial N}{\partial t}, \quad (6)$$

$$\frac{\partial^2 T}{\partial x^2} + \frac{E_g}{\tau} N - \gamma_t T_o \frac{\partial^2 u}{\partial t \partial x} = \rho c_e \frac{\partial T}{\partial t}. \quad (7)$$

$$\sigma_{xx} = (\lambda + 2\mu) \frac{\partial u}{\partial x} - \gamma_t T - \gamma_n N, \quad (8)$$

## 3 Applications

The problem initial conditions are defined as

$$u(x, 0) = 0, \frac{\partial u(x, 0)}{\partial t} = 0, T(x, 0) = 0, \frac{\partial T(x, 0)}{\partial t} = 0, N(x, 0) = 0, \frac{\partial N(x, 0)}{\partial t} = 0, \quad (9)$$

While the problem boundary conditions are given as

$$u(0, t) = 0, \tag{10}$$

$$T(0, t) = T_1 e^{-\Omega t}, \tag{11}$$

$$D_e \left. \frac{\partial N(x,t)}{\partial x} \right|_{x=0} = s_b N(x, t), \tag{12}$$

Now, for appropriateness, the dimensionless physical fields can be given by

$$N' = \frac{N}{n_o}, T' = \frac{T}{T_o}, \sigma'_{xx} = \frac{\sigma_{xx}}{\lambda+2\mu}, (x', u') = \eta c(x, u), (t', \tau') = \eta c^2(t, \tau), T'_1 = \frac{T_1}{T_o}, \Omega' = \frac{\Omega}{\eta c^2}, \tag{13}$$

where  $c^2 = \frac{\lambda+2\mu}{\rho}$  and  $\eta = \frac{\rho c_e}{K}$ .

By using the variables of nondimensional forms (13), the basic relations with the neglecting of the stars can be written by:

$$\frac{\partial^2 u}{\partial x^2} - r_1 \frac{\partial N}{\partial x} - r_2 \frac{\partial T}{\partial x} = \frac{\partial^2 u}{\partial t^2}, \tag{14}$$

$$\frac{\partial^2 N}{\partial x^2} - \frac{r_3}{\tau} N + \frac{\beta}{\tau} T = r_3 \frac{\partial N}{\partial t}, \tag{15}$$

$$\frac{\partial^2 T}{\partial x^2} + \frac{r_4}{\tau} N - r_5 \frac{\partial^2 u}{\partial t \partial x} = \frac{\partial T}{\partial t}. \tag{16}$$

$$\sigma_{xx} = \frac{\partial u}{\partial x} - r_1 N - r_2 T, \tag{17}$$

$$u(0, t) = 0, \left. \frac{\partial N(x,t)}{\partial x} \right|_{x=0} = x_6 N(0, t), T(0, t) = T_1 e^{-\Omega t}, \tag{18}$$

where  $r_1 = \frac{n_o \gamma_n}{\lambda+2\mu}$ ,  $r_2 = \frac{T_o \gamma_t}{\lambda+2\mu}$ ,  $r_3 = \frac{1}{\eta D_e}$ ,  $\beta = \frac{k T_o}{n_o \eta^2 c^2 D_e}$ ,  $r_4 = \frac{n_o E_g}{\rho c_e T_o}$ ,  $r_5 = \frac{\gamma_t}{\rho c_e}$  and  $r_6 = \frac{s_o}{\eta c D_e}$ .

### 4 Numerical Method

The basic relations obtained are linear partial differential equations. For the solutions problem, the implicit finite difference method (IFDM) is used. The solutions domain  $0 \leq x \leq x_f$ ,  $0 \leq t \leq t_f$ , are replaced by grids described by the set of nodes points  $(x_m, t_s)$ , in which  $x_m = mh$ ,  $m = 0, 1, 2, \dots, M$  and  $t_s = sk$ ,  $s = 0, 1, 2, \dots, S$ . Therefore,  $k = \frac{t_f}{S}$ ,  $h = \frac{x_f}{M}$  are taken as the time step and mesh width respectively. For the time derivatives and the space derivatives, the derivatives are replaced the central differences. Thus, the approximations of finite difference method for the system of partial differential equations with respect to the independent variables:

$$\frac{\partial f}{\partial t} = \frac{f_m^{s+1} - f_m^{s-1}}{2k} + o(k^2), \frac{\partial^2 f}{\partial t^2} = \frac{f_m^{s+1} - 2f_m^s + f_m^{s-1}}{k^2} + o(k^2), \tag{19}$$

$$\frac{\partial f}{\partial x} = \frac{f_{m+1}^{s+1} - f_{m-1}^{s+1}}{2h} + o(h^2), \frac{\partial^2 f}{\partial x^2} = \frac{f_{m+1}^{s+1} - 2f_m^{s+1} + f_{m-1}^{s+1}}{h^2} + o(h^2), \tag{20}$$

The equations (14), (15), (16) and (17) are then replaced by the implicit finite difference equations by

$$\frac{u_{m+1}^{s+1} - 2u_m^{s+1} + u_{m-1}^{s+1}}{h^2} - r_1 \frac{N_{m+1}^{s+1} - N_{m-1}^{s+1}}{2h} - r_2 \frac{T_{m+1}^{s+1} - T_{m-1}^{s+1}}{2h} - \frac{u_m^{s+1} - 2u_m^s + u_m^{s-1}}{k^2} = 0, \tag{21}$$

$$\frac{N_{m+1}^{s+1} - 2N_m^{s+1} + N_{m-1}^{s+1}}{h^2} - \frac{r_3}{\tau} N_m^{s+1} + \frac{\beta}{\tau} T_m^{s+1} - r_3 \frac{N_m^{s+1} - N_m^{s-1}}{2k} = 0, \tag{22}$$

$$\frac{T_{m+1}^{s+1} - 2T_m^{s+1} + T_{m-1}^{s+1}}{h^2} + \frac{r_4}{\tau} N_m^{s+1} - r_5 \frac{f_{m+1}^{s+1} - f_{m-1}^{s+1} + f_{m-1}^{s-1} - f_{m-1}^s}{4hk} - \frac{T_m^{s+1} - T_m^{s-1}}{2k} = 0. \tag{23}$$

$$\sigma_{xx} = \frac{u_{m+1}^s - u_{m-1}^s}{2h} - r_1 N_m^s - r_2 T_m^s. \tag{24}$$

### 5 Analytical Method

Applying the Laplace transforms for relations (14)-(18) are defined by the formula

$$\bar{f}(x, p) = L[f(x, t)] = \int_0^\infty f(x, t) e^{-pt} dt, p > 0. \tag{25}$$

Hence, the following system are obtained

$$\frac{d^2 \bar{u}}{dx^2} = p^2 \bar{u} + r_1 \frac{d\bar{N}}{dx} + r_2 \frac{d\bar{T}}{dx}, \tag{26}$$

$$\frac{d^2 \bar{N}}{dx^2} = r_3 \left( p + \frac{1}{\tau} \right) \bar{N} - \frac{\beta}{\tau} \bar{T}, \tag{27}$$

$$\frac{d^2 \bar{T}}{dx^2} = p\bar{T} - \frac{x_4}{\tau} \bar{N} + r_5 p \frac{d\bar{u}}{dx}. \tag{28}$$

$$\bar{\sigma}_{xx} = \frac{d\bar{u}}{dx} - r_1 \bar{N} - r_2 \bar{T}, \tag{29}$$

$$\bar{u}(0, t) = 0, \left. \frac{d\bar{N}(x,t)}{dx} \right|_{x=0} = r_6 \bar{N}(0, t), \bar{T}(0, t) = \frac{1}{p+\Omega}, \tag{30}$$

Now, we can use the eigenvalues method proposed [34-39] to get the solution of coupled differential equations (26), (27) and (28) with the boundary conditions (30). Hence, the matrices-vectors can be expressed as

$$\frac{dV}{dx} = AV, \tag{31}$$

where  $V = \left[ \bar{u} \quad \bar{N} \quad \bar{T} \quad \frac{d\bar{u}}{dx} \quad \frac{d\bar{N}}{dx} \quad \frac{d\bar{T}}{dx} \right]^T$  and

$$A = \begin{bmatrix} 0 & 0 & 0 & 1 & 0 & 0 \\ 0 & 0 & 0 & 0 & 1 & 0 \\ 0 & 0 & 0 & 0 & 0 & 1 \\ a_{41} & 0 & 0 & 0 & a_{45} & a_{46} \\ 0 & a_{52} & a_{53} & 0 & 0 & 0 \\ 0 & a_{62} & a_{63} & a_{64} & 0 & 0 \end{bmatrix},$$

with

$$a_{41} = p^2, \quad a_{45} = r_1, \quad a_{46} = r_2, \quad a_{52} = r_3 \left( p + \frac{1}{t} \right), \quad a_{53} = -\frac{\beta}{\tau}, \quad a_{62} = -\frac{r_4}{\tau}, \quad a_{63} = p, \quad a_{64} = pr_5.$$

The characteristic relation of matrix  $A$  can be given by

$$\xi^6 - x_3 \xi^4 + x_2 \xi^2 + x_1 = 0, \tag{32}$$

where

$$\begin{aligned} x_1 &= a_{62}a_{53}a_{41} - a_{41}a_{63}a_{52}, \\ x_2 &= a_{46}a_{52}a_{64} + a_{41}a_{52} - a_{45}a_{53}a_{64} + a_{41}a_{63} - a_{53}a_{62} + a_{52}a_{63}, \\ x_3 &= a_{46}a_{64} + a_{52} + a_{41} + a_{63}. \end{aligned}$$

The matrix eigenvalues of  $A$  are the three roots of equation (32) which define by the forms  $\pm \xi_1, \pm \xi_2, \pm \xi_3$ . Thus, the eigenvectors  $X$  are computed as:

$$\begin{aligned} X_1 &= a_{46}(a_{52} - \xi^2)\xi - \xi a_{53}a_{45}, \\ X_2 &= (a_{41} - \xi^2)a_{53}, \\ X_3 &= -(a_{41} - \xi^2)(a_{52} - \xi^2), \\ X_4 &= \xi X_1, \quad X_5 = \xi X_2, \quad X_6 = \xi X_3. \end{aligned} \tag{33}$$

Thus, the equations (31) have the solutions in the following form:

$$V(x, p) = \sum_{i=1}^3 (B_i X_i e^{-\xi_i x} + B_{i+1} X_{i+1} e^{\xi_i x}), \tag{34}$$

Due to the regularity conditions of the solution, the exponential increasing nature in the spatial variable  $x$  has been removed to infinity, therefore the final solutions of equation (31) can be written as

$$V(x, p) = \sum_{i=1}^3 B_i X_i e^{-\xi_i x}, \tag{35}$$

where  $B_1, B_2$  and  $B_3$  are constants which can be computed by the problem boundary conditions. Hence, the solutions of all variables can be presented the following forms:

$$\bar{u}(x, p) = \sum_{i=1}^3 B_i U_i e^{-\xi_i x}, \tag{36}$$

$$\bar{N}(x, p) = \sum_{i=1}^3 B_i N_i e^{-\xi_i x}, \tag{37}$$

$$\bar{T}(x, p) = \sum_{i=1}^3 B_i T_i e^{-\xi_i x}, \tag{38}$$

### 6 Numerical Results and Discussions

For numerical example, magnesium material was selected for numerical estimation purposes. The values of parameters for silicon (Si) material are taken as in [40]:

$$\begin{aligned} T_o &= 300(k), \quad \mu = 5.46 \times 10^{10}(N)(m^{-2}), \quad d_n = -9 \times 10^{-31}(m^3), \quad \lambda = 3.64 \times 10^{10}(N)(m^{-2}), \\ \alpha_t &= 3 \times 10^{-6}(k^{-1}), \quad E_g = 1.11 (eV), \quad c_e = 695(J)(kg^{-1})(k^{-1}), \quad \rho = 2330(kg)(m^{-3}), \\ T_1 &= 1, \quad \tau = 5 \times 10^{-5}(s), \quad D_e = 2.5 \times 10^{-3}(m^2)(s^{-1}), \quad s_o = 2 (m)(s^{-1}), \quad n_o = 10^{20}(m^{-3}). \end{aligned}$$

The numerical inversion method adopted the final solutions of the temperature, the displacement, the carrier density and the stress distributions. The Stehfest approach [41] can be given by

$$f(x, t) = \frac{\ln(2)}{t} \sum_{n=1}^G V_n \bar{f} \left( x, n \frac{\ln(2)}{t} \right), \tag{39}$$

With

$$V_n = (-1)^{\left(\frac{G}{2}+1\right)} \sum_{p=\frac{n+1}{2}}^{\min\left(n, \frac{G}{2}\right)} \frac{(2p)! p^{\left(\frac{G}{2}+1\right)}}{p!(n-p)! \left(\frac{G}{2}-p\right)! (2n-1)!},$$

where  $G$  is the term numbers. The field quantities, carrier density, displacement, temperature and stress depend not only on the time  $t$  and space  $x$ , but also depend on the exponent of the decayed heat flux  $\Omega$ . The numerical calculations are carried out for the time  $t = 0.4$  and  $T_1 = 1$ . Based on the above data, the variations of physical quantities along the distance  $x$  under the coupled model of thermoelastic and plasma waves are presented in figures 1–4. Figures 1 show the carrier density variation with respect to the distances  $x$ . It is observed that the carrier density begins with its maximum value on the surface  $x = 0.0$  then the carrier density decreases gradually with the increasing of the distance  $x$  till it reach to zero value. Figures 2 display the temperature variations along the distances  $x$ . It is observed that the temperature has maximum values on the surface  $x = 0.0$  then the temperature decreases with the increasing of the distance  $x$  till it closes to zero.

Figures 3 depict the displacement variations with respect to the distances  $x$ . It is observed that the displacement start from the zeros values which satisfy the problem boundary condition of on the surface  $x = 0.0$  after that it progressively increases up to peak values then decreases progressively with the rising of the distance  $x$  till it reach to zeros values. Figures 4 show the stress variations with respect to the distance  $x$ . It is observed that it attains some negative values then the magnitudes of stress gradually increase up to peak negative values after ththat the stress gradually increases to zeros values. The compressions between the solutions, one can conclude that considering the coupled photo-thermal model have major effects on the physical quantities distributions. The increasing of the exponent of the decayed heat flux  $\Omega$  reduces to the physical quantities magnitudes. Otherwise, figures 1-4 illustrates the solutions obtained numerically by the implicit finite difference method (IFDM) overlaid onto the solutions obtained analytically. The accuracy of the implicit finite.

Difference method (IFDM) formulation was validated by comparing the analytical and numerical solutions for the field quantities.

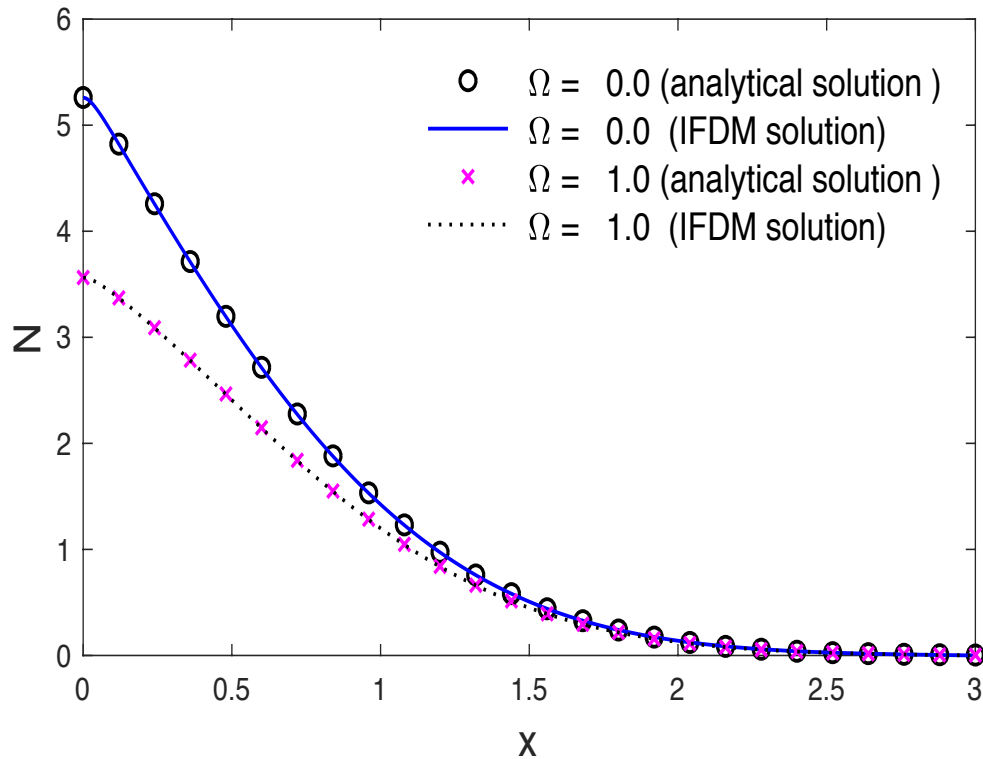


**Fig. 1:** The carrier density variations along the distance.

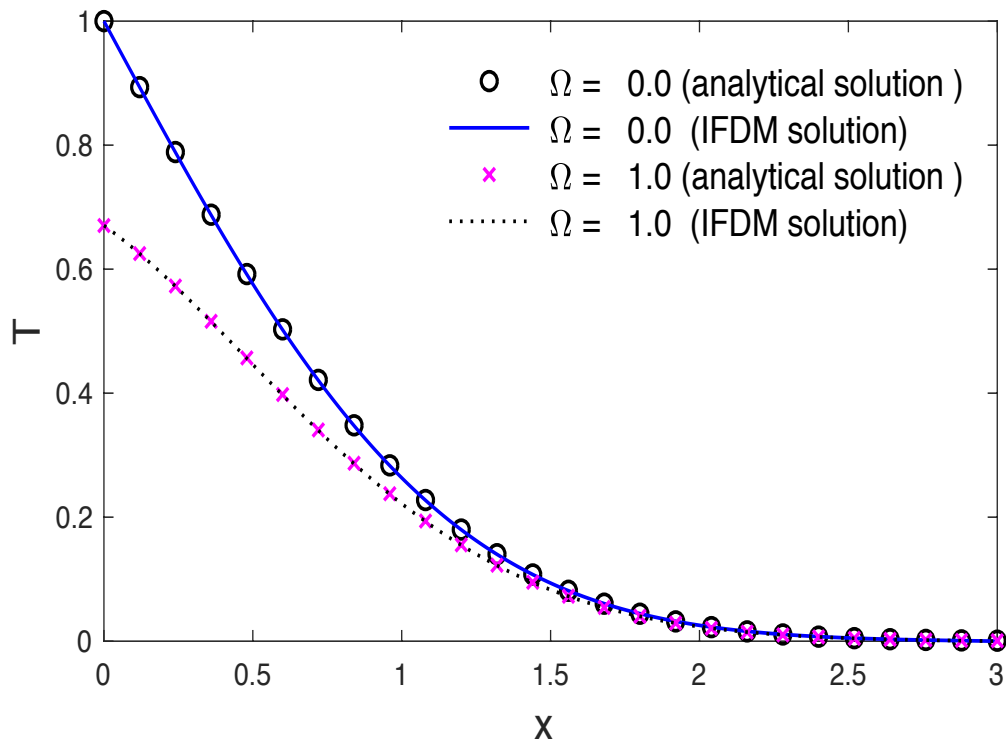


**Fig. 2:** The temperature variation along the distance.

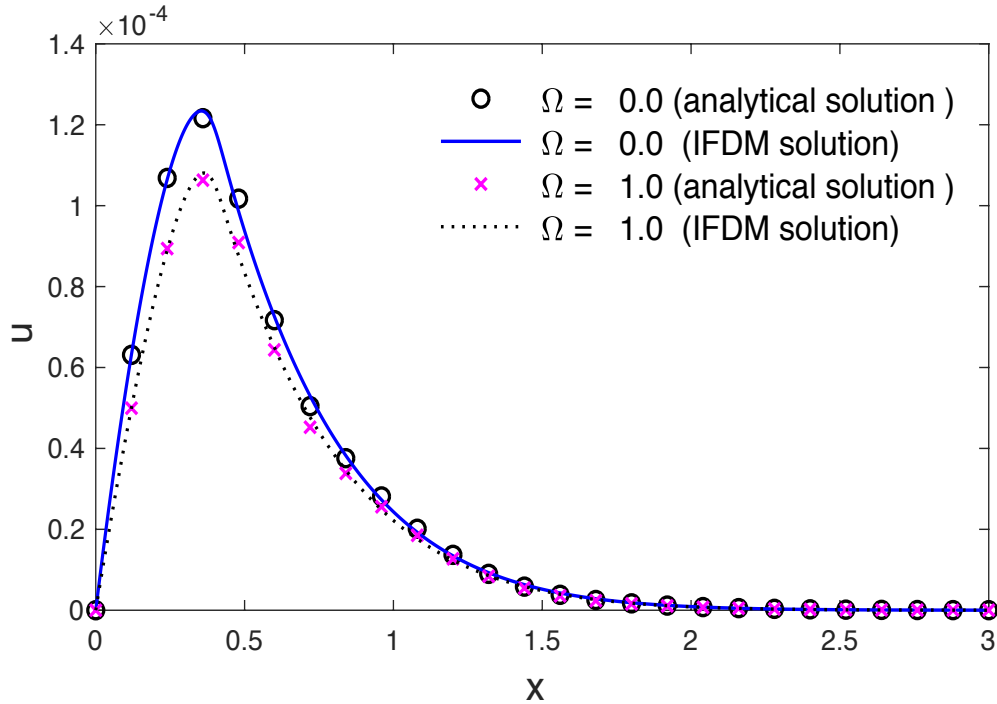


Fig. 3 The displacement variation along the distances.

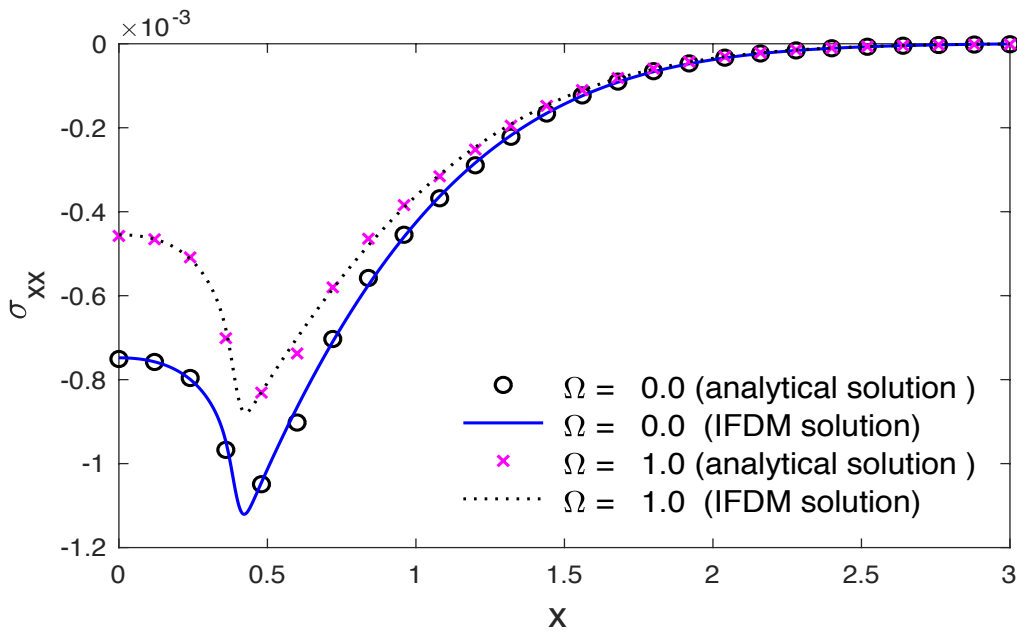


Fig. 4: the stress variations with respect to the distance.

**Conflict of interest**

The authors have no conflicts of interest to disclose.

**Acknowledgment**

This work was funded by the Academy of Scientific Research and Technology, Egypt, under Science UP grant No. (6473). The authors, therefore, acknowledge with thanks the Academy of Scientific Research and Technology for financial support.



## References

- [1] Todorović, D., Photothermal and electronic elastic effects in microelectromechanical structures. Review of scientific instruments., **74(1)**, 578-581(2003).
- [2] Todorović, D., Plasma, thermal, and elastic waves in semiconductors. Review of scientific instruments., **74(1)**, 582-585(2003).
- [3] Song, Y., et al., Study of photothermal vibrations of semiconductor cantilevers near the resonant frequency. Journal of Physics D: Applied Physics., **41(15)**, 155-106(2008).
- [4] Abd-Alla, A., et al., An implicit finite-difference method for solving the transient coupled thermoelasticity of an annular fin. Appl. Math. Inf. Sci., **1(1)**, 79-93(2007).
- [5] Mukhopadhyay, S. and R. Kumar, Solution of a problem of generalized thermoelasticity of an annular cylinder with variable material properties by finite difference method. Computational Methods in Science and Technology., **15(2)** 169-176(2009).
- [6] Abd-Alla, A., A. El-Naggar, and M. Fahmy, Magneto-thermoelastic problem in non-homogeneous isotropic cylinder. Heat and Mass transfer., **39(7)**, 625-629(2003).
- [7] Patra, S., G. Shit, and B. Das, Computational model on magnetothermoelastic analysis of a rotating cylinder using finite difference method. Waves in Random and Complex Media., 1-18(2020).
- [8] Abd-Alla, A.M., S.M. Abo-Dahab, and A.A. Kilany, Finite difference technique to solve a problem of generalized thermoelasticity on an annular cylinder under the effect of rotation. Numerical Methods for Partial Differential Equations.
- [9] Lotfy, K., et al., Response of electromagnetic and Thomson effect of semiconductor medium due to laser pulses and thermal memories during photothermal excitation. Results in Physics., **16**, 102877(2020).
- [10] Abbas, I., A. Hobiny, and M. Marin, Photo-thermal interactions in a semi-conductor material with cylindrical cavities and variable thermal conductivity. Journal of Taibah University for Science., **14(1)**, 1369-1376(2020).
- [11] Alzahrani, F., The Effects of Variable Thermal Conductivity in Semiconductor Materials Photogenerated by a Focused Thermal Shock. Mathematics., **8(8)**, 1230(2020).
- [12] Lotfy, K., A. El-Bary, and R. Tantawi, Effects of variable thermal conductivity of a small semiconductor cavity through the fractional order heat-magneto-photothermal theory. The European Physical Journal Plus., **134(6)**, 280(2019).
- [13] Lotfy, K., et al., Electromagnetic and Thomson effects during photothermal transport process of a rotator semiconductor medium under hydrostatic initial stress. Results in Physics., **16**, 102-983(2020).
- [14] Hobiny, A. and I. Abbas, A GN model on photothermal interactions in a two-dimensions semiconductor half space. Results in Physics., **15**, 102588(2019).
- [15] Alzahrani, F.S. and I.A. Abbas, Photo-thermo-elastic interactions without energy dissipation in a semiconductor half-space. Results in Physics., **15**, 102805(2019).
- [16] Abbas, I.A., The effects of relaxation times and a moving heat source on a two-temperature generalized thermoelastic thin slim strip. Canadian Journal of Physics., **93(5)**, 585-590(2014).
- [17] Zenkour, A.M. and I.A. Abbas, A generalized thermoelasticity problem of an annular cylinder with temperature-dependent density and material properties. International Journal of Mechanical Sciences., **84**, 54-60(2014).
- [18] Abbas, I.A., Nonlinear transient thermal stress analysis of thick-walled FGM cylinder with temperature-dependent material properties. Meccanica., **49(7)**, 1697-1708(2014).
- [19] Lotfy, K., Effect of variable thermal conductivity during the photothermal diffusion process of semiconductor medium. Silicon., **11(4)**, 1863-1873(2019).
- [20] Lotfy, K., et al., Thermomechanical Response Model on a Reflection Photothermal Diffusion Waves (RPTD) for Semiconductor Medium. Silicon., 1-11(2019).
- [21] Hobiny, A. and I. Abbas, Fractional Order GN Model on Photo-Thermal Interaction in a Semiconductor Plane. Silicon., 1-8(2019).
- [22] Abbas, I.A. and M. Marin, Analytical solution of thermoelastic interaction in a half-space by pulsed laser heating. Physica E: Low-dimensional Systems and Nanostructures., **87**, 254-260(2017).
- [23] Riaz, A., et al., Study of heat and mass transfer in the Eyring–Powell model of fluid propagating peristaltically through a rectangular compliant channel. Heat Transfer Research., **50(16)**, (2019).
- [24] Bhatti, M., et al., Numerical study of heat transfer and Hall current impact on peristaltic propulsion of particle-fluid suspension with compliant wall properties. Modern Physics Letters B., **33(35)**, 1950439(2019).
- [25] Marin, M., et al., On the partition of energies for the backward in time problem of thermoelastic materials with a dipolar structure. Symmetry., **11(7)**, 863(2019).
- [26] Itu, C., et al., Improved rigidity of composite circular plates through radial ribs. Proceedings of the Institution of Mechanical Engineers, Part L: Journal of Materials: Design and Applications., **233(8)**, 1585-1593(2019).
- [27] Marin, M., R. Ellahi, and A. Chirilă, On solutions of Saint-Venant's problem for elastic dipolar bodies with voids. Carpathian journal of Mathematics., **33(2)**, 219-232(2017).
- [28] Marin, M., Lagrange identity method for microstretch thermoelastic materials. Journal of Mathematical Analysis and Applications., **363(1)**, 275-286(2010).
- [29] El-Naggar, A., et al., On the initial stress, magnetic field, voids and rotation effects on plane waves in generalized thermoelasticity. Journal of Computational and Theoretical Nanoscience., **10(6)**, 1408-1417(2013).
- [30] Palani, G. and I. Abbas, Free convection MHD flow with thermal radiation from an impulsively-started vertical plate. Nonlinear Analysis: Modelling and Control., **14(1)**, 73-

- 84(2009).
- [31] Song, Y., J. Bai, and Z. Ren, Study on the reflection of photothermal waves in a semiconducting medium under generalized thermoelastic theory. *Acta Mechanica.*, 223(7), 1545-1557(2012).
- [32] Mandelis, A., M. Nestoros, and C. Christofides, Thermo-electronic-wave coupling in laser photothermal theory of semiconductors at elevated temperatures. *Optical Engineering.*, **36(2)**, 459-468(1997).
- [33] Youssef, H.M. and A.A. El-Bary, THEORY OF HYPERBOLIC TWO-TEMPERATURE GENERALIZED THERMOELASTICITY. *Materials Physics and Mechanics.*, **40**,158-171(2018).
- [34] Das, N.C., A. Lahiri, and R.R. Giri, Eigenvalue approach to generalized thermoelasticity. *Indian Journal of Pure and Applied Mathematics.*, **28(12)**,1573-1594(1997).
- [35] Abbas, I.A., Eigenvalue approach in a three-dimensional generalized thermoelastic interactions with temperature-dependent material properties. *Computers & Mathematics with Applications.*, **68(12)**, 2036-2056(2014).
- [36] Abbas, I.A., Eigenvalue approach for an unbounded medium with a spherical cavity based upon two-temperature generalized thermoelastic theory. *Journal of Mechanical Science and Technology.*, **28(10)**, 4193-4198(2014).
- [37] Abbas, I.A., A dual phase lag model on thermoelastic interaction in an infinite fiber-reinforced anisotropic medium with a circular hole. *Mechanics Based Design of Structures and Machines.*, **43(4)**, 501-513(2015).
- [38] Abbas, I.A., The effects of relaxation times and a moving heat source on a two-temperature generalized thermoelastic thin slim strip. *Canadian Journal of Physics.*, **93(5)**, 585-590(2015).
- [39] Lahiri, A., B. Das, and S. Sarkar. Eigenvalue approach to thermoelastic interactions in an unbounded body with a spherical cavity. in *Proceedings of the World Congress on Engineering*. 2010.
- [40] Song, Y., et al., Bending of Semiconducting Cantilevers Under Photothermal Excitation. *International Journal of Thermophysics.*, **35(2)**, 305-319(2014).
- [41] Stehfest, H., Algorithm 368: Numerical inversion of Laplace transforms [D5]. *Communications of the ACM.*, **13(1)**, 47-49(1970).
-